Micro-stereotactic frame utilizing bone cement for individual fabrication. An initial investigation of its accuracy.

Thomas S. Rau[*a], G. Jakob Lexow[a], Denise Blume[a], Marcel Kluge[a], Thomas Lenarz[a], Omid Majdani[a]
[a]Department of Otolaryngology and Cluster of Excellence "Hearing4all", Hannover Medical School, Carl-Neuberg-Straße 1, 30625 Hannover, Germany

ABSTRACT

A new method for template-guided cochlear implantation surgery is proposed which has been developed to create a minimally invasive access to the inner ear. A first design of the surgical template was drafted, built, and finally tested regarding its accuracy. For individual finalization of the micro-stereotactic frame bone cement is utilized as this well-known and well-established material suggests ease of use as well as high clinical acceptance and enables both sterile and rapid handling. The new concept includes an alignment device, based on a passive hexapod with manually adjustable legs for temporary fixation of the separate parts in the patient-specific pose until the bone cement is spread and finally cured. Additionally, a corresponding evaluation method was developed to determine the accuracy of the micro-stereotactic frame in some initial experiments. In total 18 samples of the surgical template were fabricated based on previously planned trajectories. The mean positioning error at the target point was 0.30 mm with a standard deviation of 0.25 mm.

Keywords: micro-stereotactic frame, surgical template, minimally invasive cochlear implantation surgery, bone cement, positioning error, accuracy

1. DESCRIPTION OF PURPOSE

Minimally invasive cochlear implantation surgery requires an accurate surgical assistance device to support the surgeon during the drilling of a single bore hole through the mastoid towards the inner ear (cochlea). Within the last decade different concepts have been described including different designs of micro-stereotactic frames. These systems are designed for direct fixation on the patient's skull close to the desired access path from the skull surface down to the cochlea. An essential aspect is the rapid and patient-specific fabrication of these surgical templates—ideally under sterile conditions while the patient is under general anaesthesia. There are systems using 3D-printing technology[1] or a CNC milling machine[2,3] for individualization of the templates. However, template fabrication using these technologies is not yet possible under sterile conditions. In contrast, Kratchman and Fitzpatrick presented a system with four legs, each consisting of several parts, which needs to be assembled in a patient-specific pose using sterile superglue[4]. Finally, Vollmann et al. introduced a micro-stereotactic frame with three initially flexible legs whose shape needs to be customized to align the frame with the planned trajectory[5]. To enable sterile shape-setting, the inventors suggest legs consisting of silicone hoses which are filled with bone cement for permanent fixation of the pose. In this study an alternative method for template-guided cochlear implantation surgery is proposed. We also utilized bone cement for rapid fabrication of the surgical template as it is a material which is well-known to medical professionals, easy to use, sterile and hardens within a few minutes.

2. MATERIALS AND METHODS

2.1 Description of the micro-stereotactic frame and its desired application

In the first step of the envisaged surgical workflow a uniform reference frame has to be attached to the patient's skull (Figure 1a). The current prototype can be bone anchored using three small self-tapping bone screws (Max Drive Drill Free 2.0x9, KLS Martin Group, Tuttlingen, Germany). The reference frame is equipped with a definite mechanical

[*] rau.thomas@mh-hannover.de; phone: +49 511 532 3025; www.mh-hannover.de/hno.html

Medical Imaging 2017: Image-Guided Procedures, Robotic Interventions, and Modeling, edited by Robert J. Webster III, Baowei Fei, Proc. of SPIE Vol. 10135, 101350P · © 2017 SPIE
CCC code: 1605-7422/17/$18 · doi: 10.1117/12.2254304

Downloaded From: http://proceedings.spiedigitallibrary.org/ on 03/20/2017 Terms of Use: http://spiedigitallibrary.org/ss/termsofuse.aspx

coupling interface (MCI) on its top. The MCI is defined by the planar top face of the frame and two dowel pins. This enables accurate mounting of the individually moulded component of the surgical template without clearance. An additional screw secures the connection throughout the surgical intervention.

In a second step, the patient's head with the reference frame needs to be scanned using an intra-operative computer tomograph (CT). In this imaging data the frame serves its second purpose defining a master coordinate system (MCS) for trajectory planning (Figure 1b). Due to its visibility in CT images reference frame enables patient-to-image registration[6].

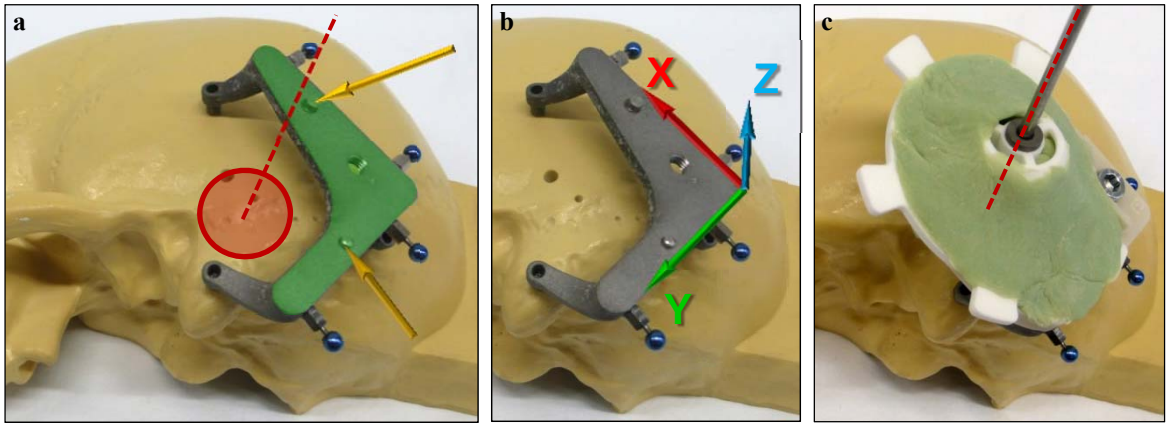

Figure 1: (a) A rigid connection between the skull of the patient (here a half-skull phantom (Sawbones Europe AB, Malmö, Sweden) is used for depiction purpose) and the surgical template is achieved due to mounting of a reference frame next to the roughly guessed entry point (red circle) of the trajectory (dotted line). The frame features a mechanical coupling interface consisting of a planar face (highlighted in green), two dowel pins (yellow arrows), and a fixation screw (shown in subfigure c). **(b)** The coupling interface defines the master coordinate system which is used for registration purposes. **(c)** The final micro-stereotactic frame is shown which incorporates the planned trajectory.

In addition to the uniform reference frame the micro-stereotactic frame has an individually mouldable component (Figure 1c). It is built up using few separate parts, which are tied by the already mentioned bone cement. These parts are disposable and will be delivered sterile to the operation room (OR). The presented prototypes have been produced out of polyamide (PA) by use of selective laser sintering (voxelwerk GmbH, Berlin, Germany). A base plate serves as counterpart to the mechanical coupling interface on top of the reference frame, enabling the assembly of the micro-stereotactic frame with high precision and repeatability. As stability of the base plate was considered a crucial aspect concerning the overall accuracy, a stiffer glass-filled PA powder was used (see Table 1). For the first prototypes a simple drill bushing (steel, hardened, according to DIN 172-B, type 4.0x16) served as linear guide.

Table 1: Listing of materials for the 3D printed component parts of the individually adjustable surgical template including their main material properties.

part	approx. dimensions [mm]	material	tensile modulus [MPa]	tensile strength [MPa]	melting temperature [°C]	heat deflection temperature [°C @ 1.80 MPa]
base plate	65 x 66 x 19	PA 3200 GF	3,200	51	176	96
subcarrier	78 x 86 x 10	PA 2200	1,650	48	176	not specified
drill bushing holder	30 x 30 x 35	PA 2200	1,650	48	176	not specified

2.2 Individualization of the surgical template

A corresponding alignment device was developed (Figure 2a) for setting the individual trajectory of the surgical template. The presented tool is based on a commercially available, passive hexapod (X1med3D, SchickDental GmbH,

Downloaded From: http://proceedings.spiedigitallibrary.org/ on 03/20/2017 Terms of Use: http://spiedigitallibrary.org/ss/termsofuse.aspx

Schemmerhofen, Germany) with manually adjustable legs. This device is marketed for the customization of surgical templates for dental implantation[7,8]. Adjusting the lengths of the hexapod's legs moves its upper platform. The original platform was replaced by a custom-made one, whose top face was equipped with a mounting plate (Figure 2b). This mounting plate features the identical mechanical coupling interface as the reference frame. Thus, the required parts of the surgical template can be temporarily aligned and fixed in the device in the same position and orientation as on the reference frame which is attached to the patient's skull. Above the upper platform an alignment pin (made of aluminium) is mounted which represents the path of the planned trajectory with respect to the template. This alignment pin fits into the drill bushing of the surgical template. Figure 2c and 2d show the alignment device loaded with the components of the surgical template during finalization of its patient-specific shape using bone cement.

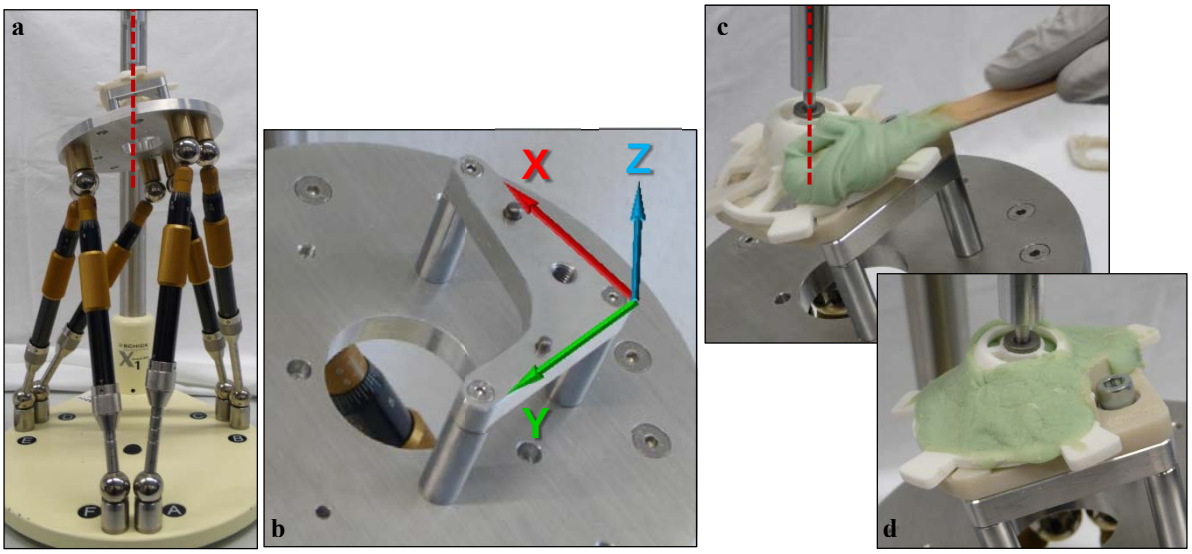

Figure 2: (a) Manually adjustable hexapod which serves for individual adjustment of the surgical template. By setting the length of each leg the upper platform can be moved with respect to an alignment pin which mimics the desired trajectory (red dashed line). **(b)** A mounting plate on top of the device, having the identical mechanical coupling interfaces, is the equivalent to the reference frame at the patient's skull. It holds the single parts of the template during the deposition of the bone cement (**c**). **(d)** Individualized surgical template after hardening of the bone cement. It is ready to be transferred to the bone anchored reference frame (compare Figure 1c).

A CAD model (Inventor Professional 2015, Autodesk, San Rafael, CA, USA) of the whole alignment device was used to calculate its specific configuration depending on the planned trajectory. This parametric assembly model is controlled by the corresponding coordinates of the start and target points. These values are stored in an Excel file (Excel 2010, Microsoft Corporation, Redmond, WA, USA) and drive the pose of the upper platform in the CAD model. In consequence also the length of each leg is updated and visualized. Finally, the measured lengths of all legs in the CAD model of the hexapod are used to manually adjust the "physical" alignment device.

After temporary pose-setting, bone cement (Palacos MV, Heraeus Medical GmbH, Wehrheim, Germany) was prepared by mixing the two components manually using a plastic bowl and a spatula. The medium viscosity enables immediate distribution over the parts of the micro-stereotactic frame to achieve a rigid connection (Figure 2c, d). No additional waiting time was necessary. First the bone cement was applied using the spatula and roughly distributed over the parts of the micro-stereotactic frame. During that time the bone cement started setting until it reached the point where it did not longer adhere to the rubber gloves. Therefore, in the second part of the moulding process the bone cement was further spread and pressed using the fingers to ensure that it infiltrated the relevant cavities of the prefabricated parts.

After the hardening of the bone cement the finished template can be demounted from the alignment device and mounted on top of the reference frame at the patient's head (Figure 1c). As a result, the finalized surgical template will guide surgical tools strictly along the planned trajectory. However, differing from the surgical workflow, in the experiments the

Downloaded From: http://proceedings.spiedigitallibrary.org/ on 03/20/2017 Terms of Use: http://spiedigitallibrary.org/ss/termsofuse.aspx

finalized surgical templates were not mounted on the reference frame but instead gauged by use of a special test bench (cf. Figure 4a and section 2.4) to determine the positioning error.

2.3 Planning and fabrication of samples

In a first trial (A) only vertical configurations were considered for an isolated investigation on how the position of the trajectory (with respect to the reference frame) influences the accuracy. It can be presumed that the more the location of the drill bushing protrudes beyond the supporting top face of the reference frame the higher the impact of deflection of the template will be on the achievable accuracy. Therefore, the starting points $P_{s,i}$ of different trajectories were spread over the possible workspace. One of these ten starting points was placed approximately in the centre of the opening of the base plate (referred to as "centre point", serving as an important reference for the second trial). As only vertical configurations were considered in trial A, the corresponding target points $P_{t,i}$ were defined as $x_{t,i} = x_{s,i}$, $y_{t,i} = y_{s,i}$, with $z_{t,i}$ = -64 mm, which equals the level of the target plane of the accuracy test bench.

The second trial (B) focussed on the impact of a maximum tilt of the trajectory on the target accuracy. Therefore, trajectories were planned starting at the centre point with a tilt of 20° from vertical. This configuration was rotated in steps of 45° around the central vertical axis resulting in eight additional samples. Consequently, the target points of these samples cover a much larger area than the samples of trial A as shown in Figure 3. In Table 2 the planned configurations for all 18 samples are summarized.

Table 2: Planned trajectories for trials A and B.

		x_s [mm]	y_s [mm]	z_s [mm]	α [°]	β [°]	x_t [mm]	y_t [mm]	z_t [mm]
trial A	#01	44.50	26.70	0.0	0.0	0.0	44.50	26.70	-64.0
	#02	24.00	36.50				24.00	36.50	
	#03	24.00	43.50				24.00	43.50	
	#04	44.40	43.70				44.40	43.70	
	#05	44.50	35.20				44.50	35.20	
	#06	33.50	32.00				33.50	32.00	
	#07	24.00	40.00				24.00	40.00	
	#08	40.00	39.00				40.00	39.00	
	#09	34.00	43.70				34.00	43.70	
	#10	37.00	36.00				37.00	36.00	
trial B	#11	37.00	36.00	0.0	20.0	0.0	60.29	36.00	-64.0
	#12					45.0	53.47	52.47	
	#13					90.0	37.00	59.29	
	#14					135.0	20.53	52.47	
	#15					180.0	13.71	36.00	
	#16					225.0	20.53	19.53	
	#17					270.0	37.00	12.71	
	#18					315.0	53.47	19.53	

For each trajectory the corresponding pose of the hexapod was calculated and set. Afterwards the base plate was assembled on the mounting plate by screwing the fixation screw hand tight. The subcarrier as well as the drill bushing holder were put on top of the base plate and aligned by inserting the alignment pin in the drill bushing. Each sample of the surgical template was finished by gluing the parts with bone cement. We did not wait until the bone cement was completely cooled down to room temperature as it reaches rigid condition while it is still lukewarm.

Downloaded From: http://proceedings.spiedigitallibrary.org/ on 03/20/2017 Terms of Use: http://spiedigitallibrary.org/ss/termsofuse.aspx

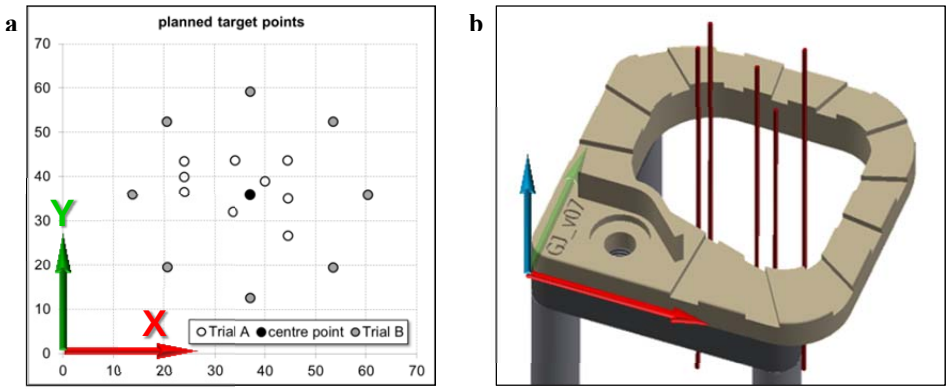

Figure 3: (a) Overview of all planned target points of both trial A (white, including the centre point in black) and trial B (grey). **(b)** Visualization of the mounted base plate (compare with Figure 2d) with some trajectories of trial A. All of them are planned vertical, which means that x- and y-coordinate of corresponding starting and target points are equal.

2.4 Determination of the positioning error

The method to measure the positioning error of the prototypes is inspired by the work of Dillon et al.[5] A test bench was built which includes a mounting plate with the identical interface as at the reference frame and at the upper platform of the alignment device (Figure 4). A metal spike was advanced through the bushing marking the reached target point with an indentation in a vinyl sheet at the base plate of the test bench. This vinyl sheet, referred to as target plate, features a grid of CNC (computerized numerical control) milled reference marks with an intermediate distance of 10 mm.

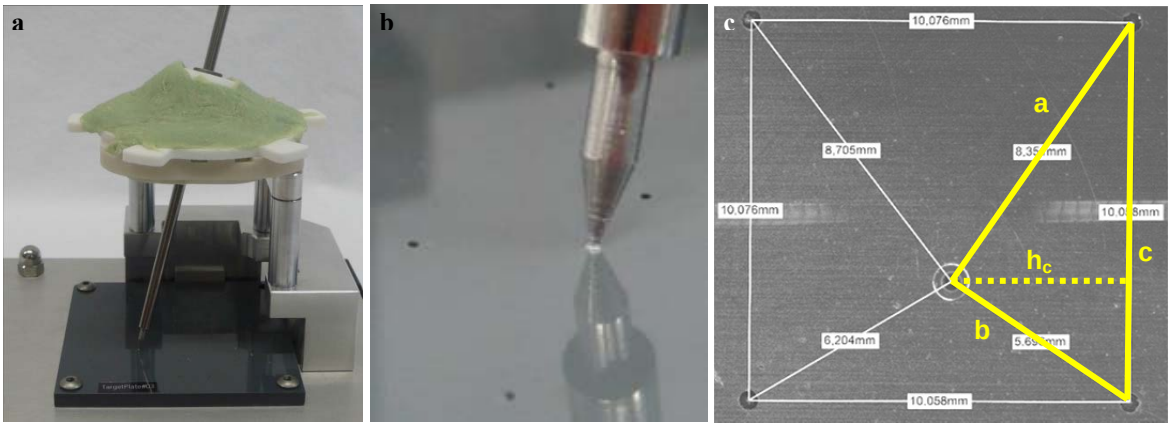

Figure 4: **(a)** Accuracy test bench with mounted template. The top surface of the target plate is 64mm below the planar top face of the MCI. **(b)** Close-up view of the pointing spike surrounded by the reference grid of the target plate marking the target point. **(c)** Microscopic image of the target point and the surrounding reference markers as well as all measured distances (one exemplary triangle is highlighted) which have been used to calculate the deviation from the planned target point.

After each trial the target plate was removed from the test bench and the position of each target mark within the reference frame was captured using a reflected-light microscope (Leica APO Z6, Leica Microsystems GmbH, Wetzlar, Germany) with full apochromatic optic (objective 0.5× Apo, Z6/Z16, f =187 mm) and a CCD camera (DFC 420, Leica Microsystems GmbH, resolution: 2,592 × 1,944 pixels). The images were captured in such way, that always both the specific target point and four surrounding reference points were visible. Image calibration was done by measuring the distances between the reference points within the image and comparing it with the well-known distances (due to the CNC-based manufacturing of the target plate) of the grid. Additionally, the distances between the target point and all four reference points were measured. Thus, for each target points four triangles exist with known lengths of sides. In Figure 4c one of these four triangles is highlighted. The altitudes from the target point within each two triangles can be

Downloaded From: http://proceedings.spiedigitallibrary.org/ on 03/20/2017 Terms of Use: http://spiedigitallibrary.org/ss/termsofuse.aspx

used to determine the actual target position both in x- and y-direction. By combining Heron's formula (1) for the area of a triangle with a formula for the area using side c as base and the altitude as height (2), the altitude h_c can be calculated with equation (3).

$$A = \sqrt{s(s-a)(s-b)(s-c)} \text{ with } s = \frac{1}{2}(a+b+c) \quad (1)$$

$$A = \frac{1}{2} \cdot c \cdot h_c \quad (2)$$

$$h_c = \frac{2}{c}\sqrt{s(s-a)(s-b)(s-c)} \text{ with } s = \frac{1}{2}(a+b+c) \quad (3)$$

Both x-values and both y-values were averaged and compared with the planned trajectory. The positioning error was defined as the Euclidean distance by which the target mark is missing the desired target point. This procedure was repeated for all samples of each trial to calculate the average error and standard deviation as well.

In order to determine the repetition accuracy (repeatability) of our method for determination of the positioning error the whole procedure was repeated twice, which included: mounting the already produced templates on top of the test bench, marking the target points with the metal spike on a new target plate, capturing images of all target points as well as measuring and calculating the target position by use of these images. The first repetitive measurement was done three days after the initial measurement; the second repetition five days later. By averaging three values for each target point we wanted to reduce the impact of random errors.

3. RESULTS

A new concept for generating a customized surgical template has been developed and the design of a first prototype was presented. Additionally, a test bench for accuracy measurements was described and used for initial trials to determine the accuracy of the newly designed micro-stereotactic frame. In total 18 samples were fabricated based on individual trajectories using the described method. Fabrication took about 20 min per sample. This includes setting the length of the hexapod's legs and hardening of the bone cement.

In the first trial (A, n = 10, only vertical configurations) the mean positioning error at the target point for all samples was 0.22 mm with a standard deviation of 0.09 mm. Details can be found in Table 3. The maximum distance to the planned target was 0.43 mm. Figure 5 shows the results of trial A, all planned target points normalized to the origin of the coordinate system.

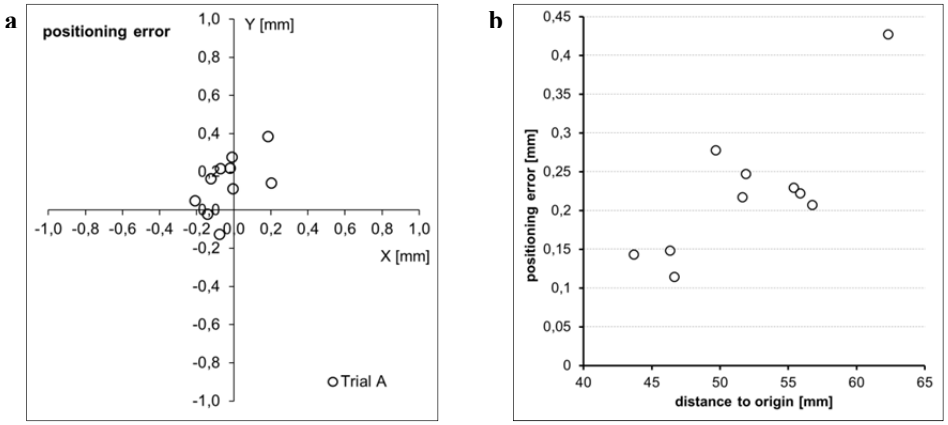

Figure 5: Results of trial A.

Downloaded From: http://proceedings.spiedigitallibrary.org/ on 03/20/2017 Terms of Use: http://spiedigitallibrary.org/ss/termsofuse.aspx

In addition the inaccuracy is visualized by plotting the positioning error against the distance of the trajectory to the origin (Figure 5b). This distance describes how much the bushing protrudes beyond the supporting reference frame. As expected the positioning error increases with decreasing support of the reference frame.

The repetitions of the measurements could not be used for averaging the results as larger deviations were observed for the second and third measurement (see Figure 6). Three and five days later the mean positioning error at the target point was 0.36 mm ± 0.20 mm and 0.37 mm ± 0.20 mm with an maximum error of 0.66 mm and 0.70 mm, respectively. This indicates that the surgical templates built with bone cement show decreasing accuracy over time. Although the differences between the second and third measurement are smaller than in comparison to the initial measurements, in some cases there are again remarkable changes in accuracy several days after producing the templates. For example, in sample #2 the positioning error increased from 0.08 mm to 0.22 mm; in contrast the error decreased from 0.35 mm down to 0.14 mm in sample #5.

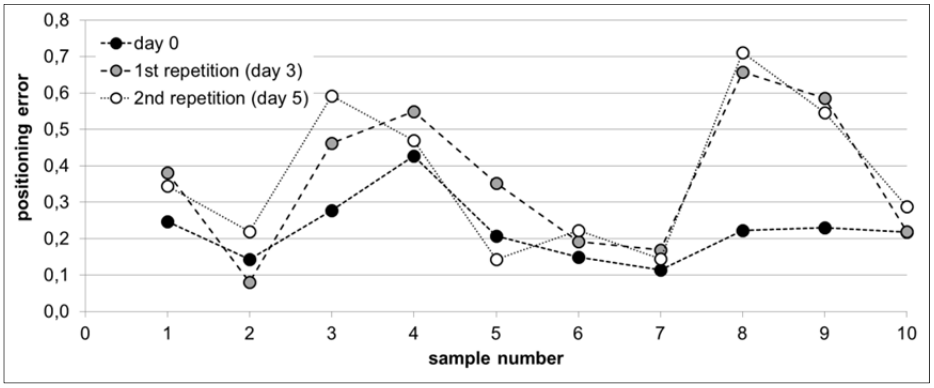

Figure 6: Change of positioning error over time for samples of trial A.

In the second trial (B, n = 8) the mean error at the target point was 0.40 mm with a standard deviation of 0.36 mm. Distribution of the error around the target point is visualized in Figure . As expected the accuracy is not as good as in trial A. The last two samples resulted in an outstanding higher inaccuracy with positioning errors of 0.70 mm and 1.15 mm. Without these outliers the mean positioning error is 0.23 mm ± 0.11 mm and close to the findings of trial A. The mean positioning error ± standard deviation of all 18 samples was found to be 0.30 mm ± 0.25 mm.

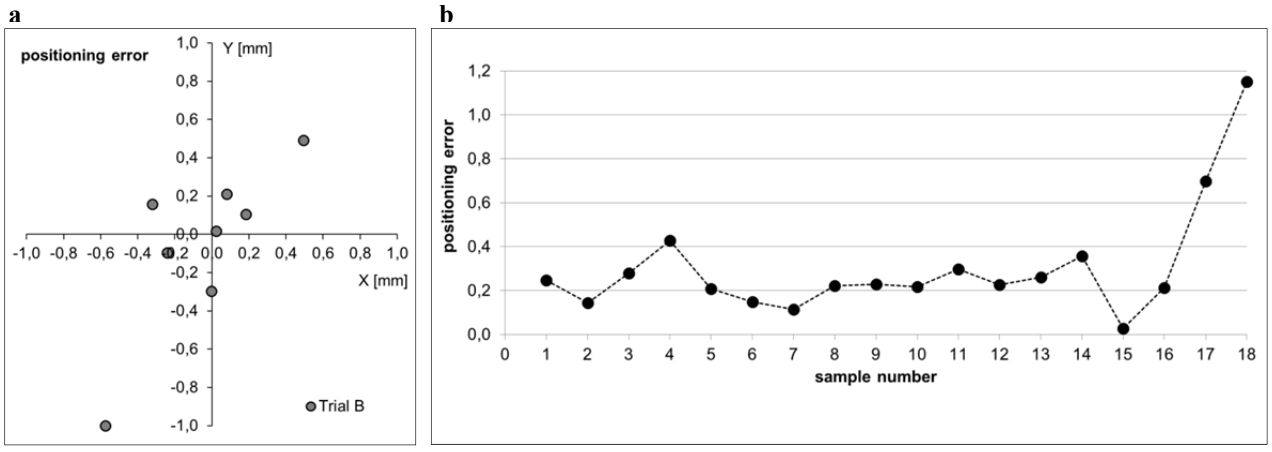

Figure 7: Results of trial B.

Downloaded From: http://proceedings.spiedigitallibrary.org/ on 03/20/2017 Terms of Use: http://spiedigitallibrary.org/ss/termsofuse.aspx

Table 3: Results of all 18 samples included in this accuracy study.

	sample	planned target		actual target		positioning error	pos. error [mm]	
		x_t [mm]	y_t [mm]	x_t [mm]	y_t [mm]	[mm]	3 days later	5 days later
trial A	#01	44.50	26.70	44.70	26.84	0.25	0.38	0.34
	#02	24.00	36.50	23.86	36.48	0.14	0.08	0.22
	#03	24.00	43.50	23.99	43.78	0.28	0.46	0.59
	#04	44.40	43.70	44.58	44.09	0.43	0.55	0.47
	#05	44.50	35.20	44.37	35.36	0.21	0.35	0.14
	#06	33.50	32.00	33.42	31.87	0.15	0.19	0.22
	#07	24.00	40.00	24.00	40.11	0.11	0.17	0.15
	#08	40.00	39.00	39.98	39.22	0.22	0.66	0.71
	#09	34.00	43.70	33.93	43.92	0.23	0.59	0.55
	#10	37.00	36.00	36.79	36.05	0.22	0.22	0.29
	mean					0.22	0.36	0.37
	SD					0.09	0.20	0.20
	max					0.43	0.66	0.71
trial B	#11	60.29	36.00	60.29	35.70	0.30		
	#12	53.47	52.47	53.55	52.68	0.23		
	#13	37.00	59.29	36.76	59.20	0.26		
	#14	20.53	52.47	20.21	52.63	0.36		
	#15	13.71	36.00	13.73	36.02	0.03		
	#16	20.53	19.53	20.71	19.63	0.21		
	#17	37.00	12.71	37.49	13.20	0.70		
	#18	53.47	19.53	52.90	18.53	1.15		
	mean					0.40		
	SD					0.36		
	max					1.15		

4. DISCUSSION AND OUTLOOK

A new concept for a micro-stereotactic frame is presented which could be used for minimally invasive cochlear implant surgery. This approach requires an accurate assistance device to support the surgeon during the drilling of a single bore hole through the mastoid towards the inner ear. Beyond the description of a first prototype and the corresponding alignment device for setting the individual trajectory of the surgical template, the average accuracy based on the experimental evaluation of at least 18 samples is presented. The mean positioning error ± standard deviation of all 18 samples was found to be 0.30 mm ± 0.25 mm. As visible in Figure 7b the last two samples of the whole study showed significantly higher position errors. After finishing the experiments and their evaluation the alignment device was investigated using a portable coordinate measuring machine (ROMER Absolute Arm Compact 7312, Hexagon Manufacturing Intelligence, Cobham, Surrey, Great Britain). We observed a distortion of the alignment pin which may explain (in parts) the large errors for sample #17 and #18. Additionally, user errors during manual adjustment of the legs of the hexapod may contribute to the total deviations. Without the last two samples the main positioning accuracy of in total 16 samples was 0.23 mm ± 0.09 mm with a maximum error of 0.43 mm, which is in the necessary submillimetre range for minimally invasive cochlear implantation surgery.

The promising results of this preliminary study endorse further research on this new micro-stereotactic frame. For clinical application user-friendly planning software will be required to provide tools for (semi-)automated segmentation, and trajectory planning. In the next step we will perform experiments using an evaluation method based on head phantoms[9] to mimic the complete surgical workflow including imaging and drilling in artificial bone material to

Downloaded From: http://proceedings.spiedigitallibrary.org/ on 03/20/2017 Terms of Use: http://spiedigitallibrary.org/ss/termsofuse.aspx

determine the accuracy and handling of the surgical template under more realistic conditions. Also an improved alignment device is currently under development which being covered in sterile drapes will enable sterile fabrication of the surgical templates. The device will show an inverse configuration with the alignment pin traversing from below through a hole in the upper platform of the hexapod. This enables an easier access to the single parts of the surgical template during deposition of bone cement.

ACKNOWLEDGEMENT

This work has been supported by the start-up grant for young researchers ‘HiLF’ of Hannover Medical School and by the German Federal Ministry of Education and Research (BMBF, FKZ 13GW0019E). Responsibility for the contents of this publication lies with the authors. The authors would like to thank D. Friedrich, A. Freimuth, and L. Uhlenbusch for their help in building the alignment device as well as in conducting the experiments.

REFERENCES

[1] Warren, F. M., Balachandran, R., Fitzpatrick, J. M. & Labadie, R. F. "Percutaneous cochlear access using bone-mounted, customized drill guides: demonstration of concept in vitro," Otol. Neurotol. 28, 325–329 (2007).

[2] Labadie, R. F., Mitchell, J., Balachandran, R. & Fitzpatrick, J. M. "Customized, rapid-production microstereotactic table for surgical targeting: description of concept and in vitro validation," Int. J. Comput. Assist. Radiol. Surg. 4, 273–80 (2009).

[3] Labadie, R. & Balachandran, R. "Clinical validation study of percutaneous cochlear access using patient customized micro-stereotactic frames," Otol. Neurotol. 31, 94–99 (2010).

[4] Kratchman, L. B. & Fitzpatrick, J. M. "Robotically-adjustable microstereotactic frames for image-guided neurosurgery," In Proc. of SPIE 8671, 86711U (2013).

[5] Vollmann, B., Müller, S., Kundrat, D., Ortmaier, T. & Kahrs, L. A. "Methods for intraoperative, sterile pose-setting of patient-specific microstereotactic frames," In Proc. of SPIE 9415, 94150M (2015).

[6] Fitzpatrick, J. M. "The role of registration in accurate surgical guidance," Proc. Inst. Mech. Eng. H. 224, 607–22 (2010).

[7] Ewers, R. et al. "Planning implants crown down- a systematic quality control for proof of concept," J. Oral Maxillofac. Surg. 68, 2868–2878 (2010).

[8] Behneke, A., Burwinkel, M., Knierim, K. & Behneke, N. "Accuracy assessment of cone beam computed tomography-derived laboratory-based surgical templates on partially edentulous patients," Clin. Oral Implants Res. 23, 137–143 (2012).

[9] Lexow, G. J., Kluge, M., Majdani, O., Lenarz, T., Rau, Th. S. "Phantom-based evaluation method for surgical assistance devices in minimally-invasive cochlear implantation," In Proc. of SPIE 10135, 10135-94 (2017).

Downloaded From: http://proceedings.spiedigitallibrary.org/ on 03/20/2017 Terms of Use: http://spiedigitallibrary.org/ss/termsofuse.aspx